Towards an Extension of the $v^2 - f$ Model for Transitional Flows

A. Sveningsson
Department of Thermo and Fluid Dynamics,
Chalmers University of Technology,
SE-412 96 Gothenburg, Sweden

October 7, 2006

Abstract

In part, this study investigates the performance of the turbulence model of Walters and Leylek (2004) in the flow over a flat plate under the influence of a disturbed freestream. The most important feature of the model is that is solves an equation for a laminar kinetic energy, which is coupled to a typical $k-\varepsilon$ model, to improve the performance in transitional flows. The model is shown to be very sensitive to the prescribed freestream turbulence length scale.

The study also describes the initial steps towards coupling the laminar kinetic energy transition modelling approach, suggested by Walters and Leylek (2004), to the $v^2 - f$ turbulence model in an effort to improve the $v^2 - f$ model's performance in transitional flow regimes. This coupling requires modifications of the $v^2 - f$ model but the intention is that the new model should retain the properties of the original model in fully turbulent boundary layers and that the additional laminar kinetic energy equation should make the predictions in transitional boundary layers more reliable.

Finally, in an initial numerical study some potential pitfalls when modelling the flat plate flow are analyzed. It is shown that the predicted transitional behavior obtained with the simplified, as compared with the experimental set-up, numerical domain used in this study may be directly compared with measurements.

1 Introduction

With the last decades of intense research in turbulence modelling statistical descriptions of turbulence are about to mature. Today closures exist that are able to provide accurate predictions of turbulence effects on the mean flow characteristics given that the mean flow itself is not too complicated. However, there is one phenomenon that can cause the most advanced turbulence model to fail in the, seemingly, most straightforward flows to compute, e.g. flow over a flat plate. This phenomenon is the transition of a laminar boundary layer into a turbulent state. With the improvements in turbulence modelling the inability to account for transitional effects has become more pronounced. The interest in developing methods aimed at extending the applicability of turbulence models to include also transitional flows has therefore grown.

The present study deals with laminar to turbulence transition of boundary layers due to elevated levels of freestream disturbances – so called bypass transition. The other two types of transition, natural transition and transition preceded by separation, will at present not be included in the model framework developed in the following sections. The reasons why bypass transition is considered are that the mechanism behind it is rather well suited for a statistical description, i.e. there is a possibility that the phenomenon can be sufficiently accurately modelled with a standard RANS-based approach, and that bypass transition is commonly encountered in gas turbine design, especially in the high pressure turbine where large levels of freestream disturbances exist.

In bypass transition freestream disturbances penetrate the boundary layer and induce low frequency fluctuations, primarily in the streamwise velocity component, u'. The fluctuations appear as long streamwise streaks within the boundary layer and after an initial growth some of the streaks eventually collapse to form so called turbulent spots. Thus, most stages in the natural transition route to turbulence are bypassed and the boundary layer transitions earlier than the boundary layer beneath an undisturbed freestream.

Much of the detailed physics behind bypass transition is still unknown. In an effort to provide the data necessary to depict the interaction of freestream turbulence with a laminar boundary layer Jacobs and Durbin (2001) performed a DNS of a flat plate flow in an environment of elevated turbulence intensity, $Tu = 3.0\%$. Their results suggest that low frequency perturbations in the freestream are able to penetrate the boundary layer, where they produce boundary layer modes of even lower frequency (the streaks mentioned above). These modes in turn are acted upon by shear and grow and elongate in the direction of the flow. When the modes have reached a certain amplitude they, as suggested by Jacobs and Durbin (2001), become receptive to wall-normal fluctuations in the freestream and turbulent spots begin to appear.

Shortly after the first two-equation turbulence models were developed it was

realized that these models could in principle be used to predict bypass transition. The well known mechanism is that freestream turbulence (i.e. k) diffuses into the boundary layer. Consequently, the computed eddy-viscosity increases and the production of additional turbulence grows. When the production reaches a certain critical level, where the turbulence dissipation no longer balances the production, the boundary layer undergoes transition.

The 'classical' way to alter the transitional behavior of RANS models is to introduce/modify the so called low Reynolds number extensions to the 'standard' versions of the models. These functions control the balance between production of turbulence and the production (and/or dissipation) of the dissipation rate of turbulence. The behavior of most low Reynolds number models are discussed in Savill (2002a), where it is concluded that models with a Launder-Sharma type of source term are among the best in terms of predicting the location of transition. Another approach taken by, e.g., Dopazo (1977), Byggstoyl and Kollmann (1981) or Steelant and Dick (1996), is the use of conditional averages. Here two sets of equations, one laminar and the other turbulent, are solved and combined using the intermittency factor, γ, to yield the total solution. In addition, a transport equation for γ is solved and the problem of triggering the production of k is replaced with the problem of triggering the production of γ, where the latter seems to rely heavily on the prescribed (non-zero) inlet boundary condition for γ itself. This weakness is not only present in models employing conditional averages but also in models where a transport equation for γ is used in conjunction with standard turbulence models, e.g. the version of the SLY (cf. Westin and Henkes (1997) for full details of this model) model given in Savill (2002b).

A rather different approach to transition modelling is that of Menter et al. (2004). Their model does in principle not rely on the prediction of the location of transition but is rather based on a transport equation for a critical Reynolds number related to the onset location of transition. The critical Reynolds number in turn is obtained from an empirical correlation (which in principle can be arbitrarily specified by the user) and thus experimental experiences can by incorporated into the transition model. A problem with the model is that some details of the model are considered proprietary.

The nature of the pretransitional boundary layer fluctuations, induced by freestream turbulence, is not turbulent. They can therefore not be expected to behave as typical turbulent fluctuations with the characteristic energy cascade and interaction with a mean shear to produce additional fluctuations. This was realized by Mayle and Schultz (1997) who proposed a transport equation for laminar kinetic energy (LKE) to describe the evolution of statistics of these non-turbulent fluctuations. They found that the unsteadiness in laminar boundary layers correlates with wall-normal fluctuations in the freestream and suggested that the laminar fluctuations are produced by a pressure-diffusion mechanism. This concept was

investigated by Lardeau et al. (2004) who performed a LES of the flow and computed budgets of the kinetic energy in the pretransitional boundary layer. They found that the growth in LKE does not owe to pressure-diffusion, which proved to act as a sink, but rather to an uv-correlation acting on a mean velocity gradient. Nevertheless, Lardeau et al. (2004) used the model of Mayle and Schultz (1997) with reasonable success to account for the effect of LKE before the onset of transition.

Walters and Leylek (2004) extended the concept of describing pretransitional boundary layers with a transport equation for laminar kinetic energy. They formulated a complete single-point RANS turbulence model that consists of not only the LKE (k_L) equation but does also include equations for turbulence kinetic energy (k_T) and its dissipation rate, ε. Using this model the transitional behavior in the flat plate experiment of Blair (1983) was successfully reproduced. Of even greater interest was the model's ability to reproduce the influence of the large variations in freestream turbulence on transitional features in the linear cascade measurements by Radomsky and Thole (2001). A weakness of the model is, as will be shown in Section 4.2, its strong sensitivity to the length scale of the freestream turbulence.

The v^2-f turbulence model, originally proposed by Durbin (1991) and based on the elliptic relaxation approach, constitutes a model that has proven to perform reasonably well in complex flows including, for example, stagnation points and flow separation. Its behavior in transitional flows like the linear cascade flow mentioned earlier is on the other hand less satisfactory (Sveningsson and Davidson, 2005). However, as the v^2-f model's performance in fully turbulent flows in general is good it would be desirable to improve its predictive capabilities also in transitional flows. This is indeed the motivation for the present study. The aim is to combine the v^2-f model with the transition modelling approach of Walters and Leylek (2004). The intention is that for fully turbulent boundary layers the model should reduce to a form close to the original v^2-f model, whereas the performance in the transitional region should be improved by solving an additional transport equation for the LKE.

2 Governing Equations and Turbulence Models

The equations governing the evolution of mean momentum of an incompressible fluid in a steady flow are given by

$$U_j \frac{\partial U_i}{\partial x_j} = -\frac{1}{\rho}\frac{\partial P}{\partial x_i} + \nu \frac{\partial^2 U_i}{\partial x_j^2} - \frac{\partial \overline{u_i u_j}}{\partial x_j} \tag{1}$$

As is always the case in RANS computations the Reynolds stresses, $\overline{u_i u_j}$, are unknown and need to be modelled with an appropriate turbulence closure. In this study the turbulence models used are the $v^2 - f$ model originally suggested by

Durbin (1991), the model of Walters and Leylek (2004) and a new model developed in the present study.

The proposed model is based on the elliptic relaxation approach (suggested by Durbin (1991)). The $v^2 - f$ turbulence model used as starting point here is identical to that described in Cokljat et al. (2003). To improve the model's performance in transitional flows a number of modifications have been introduced. Most of these modifications follow earlier work on transition modelling of Walters and Leylek (2004). The most important concept is the introduction of a transport equation for laminar (mainly pretransitional) kinetic energy (LKE). The purpose of introducing a second fluctuating energy is to allow a more accurate modelling of the effect of the fluctuations in pretransitional regions that is only weakly coupled to the turbulence kinetic energy. In other words, it is desirable to be able to modify the model's behavior in the pretransitional region without modifying its behavior in the fully turbulent region where we wish to retain the properties of the original $v^2 - f$ model. Further, as has been shown in a DNS by Jacobs and Durbin (2001), there exists some evidence that the pretransitional laminar fluctuations are precursors to the formation of turbulent spots. This inspired Walters and Leylek (2004) to create a model in which production of turbulence was triggered by the presence of laminar kinetic energy. Both the above concepts are adopted in the present study as well.

To illustrate how the different contributions to the total fluctuating energy are intended to sum up results from two flat plate computations are shown in Figure 1. The variations of different types of energies are plotted across the boundary layer just downstream of the leading edge of the plate ($Re_x \approx 15,000$). The thick solid line show the TKE of the 'standard' $v^2 - f$ model employed in this study. As this model does not involve an equation for a laminar type of fluctuation this is also the total energy predicted by this model. The other curves give the results of the Walters and Leylek (2004) model. It can be seen that the TKE (k_T) in the freestream diffuses into the boundary layer and approaches zero at the wall. This means that the production of additional TKE is balanced by the dissipation of the same when integrated over the boundary layer. The contributor responsible for the growth in total KE ($k_T + k_L$) is the LKE (k_L), which has its maximum at about half the boundary layer height. This illustrates the fundamental difference in modelling approach, i.e. that the increase in KE in the boundary layer prior to transition owes to an increase in the non-turbulent fluctuations, k_L, not to production of TKE.

Another concept of Walters and Leylek (2004) was to employ two different viscosities. The first is a 'standard' eddy, or turbulence, viscosity related to motions that are active in producing additional turbulence. This viscosity is referred to as a small scale viscosity, $\nu_{T,s}$. The second viscosity on the other hand does not contribute to the production of turbulence. Instead, by acting on a mean flow gradient, it produces laminar (most often pretransitional) kinetic energy and is

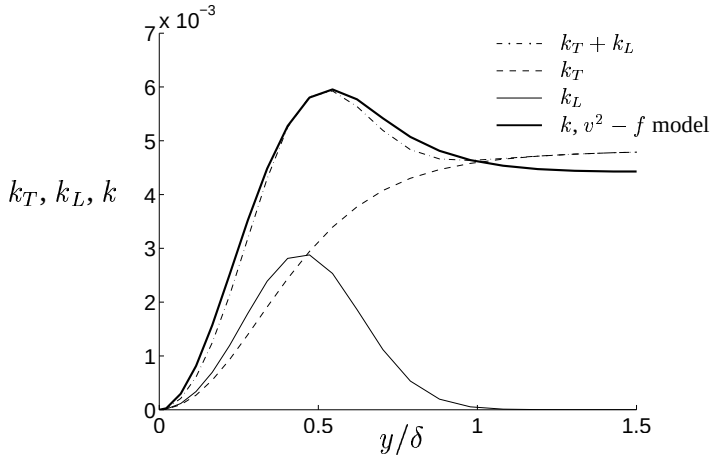

Figure 1: Profiles of the different contributors (k_L and k_T) to the total fluctuating energy, k, at a position upstream of the location of transition.

referred to as a large scale viscosity, $\nu_{T,l}$.

The LES of Lardeau et al. (2005) suggests that the main contributor to LKE growth is that of Reynolds stresses acting on a mean flow gradient. This is the same mechanism as in fully turbulent flows with the only difference that the shear to normal stress ratio ($\overline{uv}/\overline{u_i u_i}$) is some 30-50 percent lower. It is therefore believed that the approach taken by Walters and Leylek (2004), i.e. to introduce a second large scale eddy-viscosity ($\nu_{T,l}$) to model the production of LKE in analogy with TKE production, stands on reasonably firm ground.

The partial differential equations governing the $v^2 - f$ model sensitized to transition are

$$\frac{Dk_T}{Dt} = \frac{\partial}{\partial x_j}\left[\left(\nu + \frac{\nu_{T,s}}{\sigma_k}\right)\frac{\partial k_T}{\partial x_j}\right] + P_T + R - \varepsilon \quad (2)$$

$$\frac{D\tilde{\varepsilon}}{Dt} = \frac{\partial}{\partial x_j}\left[\left(\nu + \frac{\nu_{T,s}}{\sigma_\varepsilon}\right)\frac{\partial \tilde{\varepsilon}}{\partial x_j}\right] + \frac{\tilde{\varepsilon}}{k_T}\left(C_{\varepsilon 1}\left(P_T + R\right) - C_{\varepsilon 2}\varepsilon\right) \quad (3)$$

$$\frac{Dv^2}{Dt} = \frac{\partial}{\partial x_j}\left[\left(\nu + \frac{\nu_{T,s}}{\sigma_k}\right)\frac{\partial v^2}{\partial x_j}\right] + k_T f - 6\frac{v^2}{k_T}\varepsilon \quad (4)$$

$$\frac{Dk_L}{Dt} = \frac{\partial}{\partial x_j}\left[\nu\frac{\partial k_L}{\partial x_j}\right] + P_L - R - D_L \quad (5)$$

$$L^2\frac{\partial^2 f}{\partial x_j \partial x_j} - f = \frac{C_1\varepsilon}{k_T}\left(\frac{v^2}{k_T} - \frac{2}{3}\right) - C_2\frac{P_T + R}{k_T} - 5\frac{v^2}{k_T^2}\varepsilon \quad (6)$$

The main difference as compared with the original $v^2 - f$ model equations is that the standard ε equation has been replaced with an equation for $\tilde{\varepsilon} = \varepsilon - D_T$. The main purpose of this modification was to have turbulence length scales (cf. Eqn

8) in the pretransitional boundary layer similar to those predicted by the model of Walters and Leylek (2004) so that the new model also produces effective length scales in accordance with the Walters and Leylek (2004) model.

A problem with the original $v^2 - f$ model is that transition is predicted too early (Sveningsson and Davidson, 2005). In the new model the production of turbulence is decreased by introducing a damping function in the expression for turbulence production. Also worth mentioning here is that the use of different limits on the turbulence time scale has been removed and is replaced by $k/\tilde{\varepsilon}$ (or sometimes k/ε). The realizability constraint is only used when the small scale turbulence viscosity is computed.

By use of the effective length scale the turbulence kinetic energy is split into small and large scale energies, $k_{T,s}$ and $k_{T,l}$, respectively. They are computed as (Walters and Leylek, 2004)

$$\begin{aligned} k_{T,s} &= k_T \left(\frac{\lambda_{\mathit{eff}}}{\lambda_T} \right)^{2/3} \\ k_{T,l} &= k_T \left(1 - \left(\frac{\lambda_{\mathit{eff}}}{\lambda_T} \right)^{2/3} \right) \\ \lambda_T &= \frac{k_T^{3/2}}{\tilde{\varepsilon}} \end{aligned} \tag{7}$$

where the effective turbulence length scale is given by

$$\lambda_{\mathit{eff}} = \min \left(C_\lambda \frac{k}{\sqrt{\tilde{\varepsilon} S}}, \lambda_T \right), \quad S \equiv \sqrt{2 S_{ij} S_{ij}} \tag{8}$$

Here the length scale $k/\sqrt{\tilde{\varepsilon} S}$ replaces the wall distance used by Walters and Leylek (2004). The new length scale couples better with the boundary layer thickness as it is sensitized to the inverse of $S^{1/2}$ that becomes large outside the boundary layer. As will be shown later, using the wall distance when computing λ_{eff} causes the location of the length scale switch (cf. Eqn 8) to become strongly dependent on the length scale of the freestream and not at all related to the extent of the boundary layer.

As mentioned above, the production of turbulent and pretransitional fluctuating energy, k_T and k_L, respectively, is modelled using two different viscosities, i.e.

$$P_T = f_P \nu_{T,s} S^2 \tag{9}$$

$$P_L = \nu_{T,l} S^2 \tag{10}$$

The viscosities, $\nu_{T,s}$ (small scale) and $\nu_{T,l}$ (large scale) are calculated as

$$\nu_{T,s} = C_{\mu,s} v^2 T \tag{11}$$

$$\nu_{T,l} = f_{\mu,l} C_{\mu,l} \frac{\Omega \lambda_{\mathit{eff}}^2}{\nu} \sqrt{k_{T,l}} \lambda_{\mathit{eff}} \tag{12}$$

with

$$T = \frac{\lambda_{eff}}{\sqrt{k_T}} \tag{13}$$

With this definition of T the model returns essentially the same eddy-viscosity as the original $v^2 - f$ model in areas where $\lambda_{eff} = k_T^{3/2}/\varepsilon$ and the damping function $f_P \approx 1$, which ideally will happen after transition to turbulence has occurred.

A feature of the present model that differs from the model of Walters and Leylek (2004) is that the production of TKE (P_T) is dampened but not the small scale viscosity producing it. The reason is that the fluctuations (k_T) that diffuse into the boundary layer are believed to contribute to transport processes (e.g. it increases heat transfer) via the so called splat mechanism (cf. Bradshaw, 1996) and should therefore not be dampened. The freestream fluctuations on the other hand, at least initially, couple poorly with the mean velocity gradients in the boundary layer (this effect is referred to as shear sheltering, Jacobs and Durbin (2001)), and therefore the production term needs to be dampened in the pretransitional region.

The damping function, f_P, used to reduce the production is computed as

$$f_P = \min(f_1, f_2) \tag{14}$$

$$f_1 = \frac{I_T^2}{1.0 + I_L^{1/2}\left(\frac{Sk}{\tilde{\varepsilon}}\right)^2} \tag{15}$$

$$f_2 = 1.0 - \exp\left(-f_3\left(\frac{\tau_m}{\tau_{T,s}}\right)^2\right) \tag{16}$$

$$f_3 = \min\left(C_{f_{3,1}}, C_{f_{3,2}}\frac{k_T + k_L}{k_L}\right) \tag{17}$$

$$I_L = 1.0 - I_T \tag{18}$$

$$I_T = \min\left(0.2\frac{k_T f}{\varepsilon}\left(\frac{k_T}{v^2}\right)^{1.5}, 1.0\right) \tag{19}$$

The idea behind the choice of f_1 is to use the nonlocality of the flow variable f (note that $I_T = I_T(f)$). Here it is used to dampen the eddy-viscosity at around the edge of the pretransitional boundary layer (note that the effect of f_1 extends beyond the edge of the boundary layer). Further, in pretransitional regions, where the function $I_T < 1.0$ (and consequently $0 < I_L < 1$) f_1 becomes inversely proportional to $(Sk_T/\tilde{\varepsilon})^2$, which according to Pettersson-Reif et al. (1999) is a necessary condition for the model to be able to bifurcate between laminar and turbulent solutions. In fully developed turbulent channel flow the effect of f_1 is negligible as I_T is unity in turbulent boundary layers. Note that the function used in the expression for I_T reaches a value of approximately 1.2 in the homogeneous freestream (if $v^2 = 2k/3$) and is independent of freestream values of both k_T and ε. Thus, I_L serves as an indicator of non-turbulent boundary layers.

The purpose of the function f_2 is to dampen the eddy-viscosity in regions where the laminar kinetic energy is nonzero. Recall that the desired transition mechanism is that laminar kinetic energy shall trigger production of turbulence kinetic energy. Hence, the standard production mechanism is dampened where laminar energy exists. The dependence on k_L is introduced in the f_3 function. This function was given a lower limit of $C_{f_{3,1}}$ to speed up the convergence rate in cases where k_L is initially small in the boundary layer (i.e. in case of a poor initial guess). The influence of this constant on the converged solution is limited. $\tau_m \equiv 1/S$ in the expression for f_2 was chosen to have a reduced damping as the boundary layer grows. Initially, gradients (S) are large in the thin laminar boundary layer and when the boundary layer grows S is reduced and so is the dampening.

To make sure that the laminar kinetic energy disapears in fully turbulent boundary layers it was decided to dampen also the large scale viscosity using the damping function $f_{\mu,l}$, defined as

$$f_{\mu,l} = \min\left(C_I I_L^{1/2}, 1.0\right) \tag{20}$$

Here the function I_L reduces $f_{\mu,l}$ to zero as the boundary layer transitions. Recall that I_L is zero in turbulent boundary layers.

The production term coefficient, $C_{\varepsilon 1}$, in the ε equation was given the same form as in the $\overline{v^2} - f$ model, i.e.

$$C_{\varepsilon 1} = 1.4\left(1 + 0.045\sqrt{k/v^2}\right) \tag{21}$$

The destruction terms in the k_L and k_T equations are computed as

$$D_T = 2\nu \frac{\partial\sqrt{k_T}}{\partial x_j}\frac{\partial\sqrt{k_T}}{\partial x_j} \tag{22}$$

$$D_L = 2\nu \frac{\partial\sqrt{k_L}}{\partial x_j}\frac{\partial\sqrt{k_L}}{\partial x_j} \tag{23}$$

and the total dissipation rate of turbulence kinetic energy is thus $\varepsilon = \tilde{\varepsilon} + D_T$.

The Reynolds stresses, $\overline{u_i u_j}$, in Eqn 1 are modelled using the total eddy-viscosity

$$-\overline{u_i u_j} = 2\left(\nu_{T,s} + \nu_{T,l}\right) S_{ij} + \frac{2}{3} k_T \delta_{ij}, \tag{24}$$

i.e., the large scale eddy-viscosity ($\nu_{T,l}$) enhances, in the model, the mixing due to the pretransitional fluctuations. Recall that $\nu_{T,l}$ does not contribute to the production of turbulence. Note however that it is not absolutely clear how the laminar fluctuations actually influence mean flow properties such as heat transfer and momentum transport. If k_L exists only as fluctuations in u, as indicated in the DNS

studies of Jacobs and Durbin (2001) and Brandt et al. (2004), there cannot be any $\overline{uv}$ correlation to transport momentum (or heat) towards the wall. On the other hand, as shown by Lardeau et al. (2005), it is, from a statistical point of view, a shear stress/mean strain interaction that produces the laminar kinetic energy. For the same reason it is not clear that only the small scale viscosity should be used in the equations for the turbulence statistics (Eqn 2-4). Note that the large scale viscosity is considerably lower than its small scale counterpart and therefore its effect is expected to be marginal.

The turbulence length scale, L, is given by

$$L = C_L \max\left(\frac{k^{3/2}}{\varepsilon},\ C_\eta\left(\frac{\nu^{3/4}}{\varepsilon^{1/4}}\right)\right), \tag{25}$$

and the remaining model coefficients are:

$$C_{\mu 1} = 0.25;\ \ C_{\varepsilon 2} = 1.9;\ \ C_1 = 0.4;\ \ C_2 = 0.3;\ \ \sigma_k = 1.0;\ \ \sigma_\varepsilon = 1.3 \tag{26}$$

$$C_L = 0.23;\ \ C_\eta = 70;\ \ C_I = 3;\ \ C_{f_{3,1}} = 400;\ \ C_{f_{3,2}} = 50 \tag{27}$$

The transition mechanism of the proposed model is that laminar kinetic energy (k_L) shall transform into turbulence kinetic energy (k_T) and be responsible for the initial build-up of the turbulence production that eventually causes the laminar to turbulence breakdown. This scenario is modelled with the R term introduced in Eqn 2 and 5, i.e. with the same approach as of Walters and Leylek (2004). Here R is given the form

$$R = C_R \frac{k_L}{\tau_T}, \quad \tau_T = \frac{\lambda_{eff}}{\sqrt{k_T}} \tag{28}$$

Note the delicate balance between the turbulence production damping term, f_2, that involves k_L (cf. Eqn 16, large k_L/k_T ratio, large damping) and the production mechanism modelled with the R term (large k_L, large production).

3 Numerical Approach

For all computations reported here, an in-house code, CALC-BFC (Boundary Fitted Coordinates) (Davidson and Farhanieh, 1995), was employed. CALC-BFC allows use of structured meshes only and uses the SIMPLEC algorithm for the coupling of pressure to the velocity field. All data are stored at the control volume centers (co-located grid arrangement) and Rhie and Chow interpolation is used to prevent the pressure fluctuations often encountered with this approach. All equations were discretized using the van Leer scheme and the resulting sets of equations were solved with a standard segregated TDMA solver.

At the inlet uniform profiles of all quantities except for f and P were specified. The actual values of k and ε were determined by modifying these properties at the

Property/Variable	U_{in}	$k_{T,in}$	ε_{in}	ρ	μ	$k_{L,in}$
T3A	1.0	0.0294	4.535	1.0	10^{-6}	0.0
T3B	1.0	0.0096	0.0778	1.0	10^{-6}	0.0
Blair $Tu = 2.6\%$	1.0	0.00118	0.00066	1.0	10^{-6}	0.0
Blair $Tu = 6.2\%$	1.0	0.0106	0.0109	1.0	10^{-6}	0.0

Table 1: Specified inlet conditions and fluid properties.

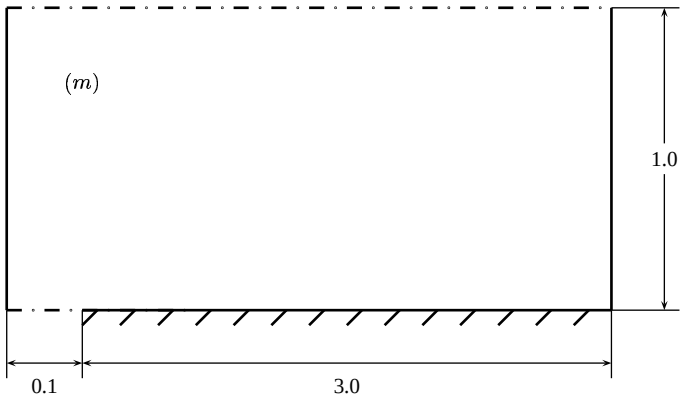

Figure 2: Schematic of the computational domain.

inlet until the freestream decays of turbulence kinetic energy of the experiments considered were matched. When used, v^2 was set to two thirds of k and for f a Neumann boundary condition was used. The actual values of specified inlet and fluid properties are given in Table 1.

The other boundary conditions for the original $v^2 - f$ model are described in e.g. Sveningsson and Davidson (2005). The boundary conditions of the modified version presented here are the same with the exception of the $\tilde{\varepsilon}$ wall boundary condition, which now simply reads $\tilde{\varepsilon}_w = 0$

Figure 2 shows a schematic of the computational domain used for the majority of the simulations. The origin of the coordinate system coincides with the leading edge of the plate. Note that the plate is assumed to be infinitely thin.

The primary mesh consisted of 217 cells in the streamwise direction with 88 cells covering the height of the domain. y^+ values were below unity for the first wall adjacent cells with the exception of a few cells immediately downstream of the leading edge. Grid spacing was used to cluster cells in the boundary layer and around the leading edge. The mesh used is shown in Figure 3 (every second grid line in both directions is shown). In the region where transition is expected to occur ($0.1 < x < 0.7$) the cell size in the streamwise direction is constant as it was found that incautious spacing may in fact trigger transition.

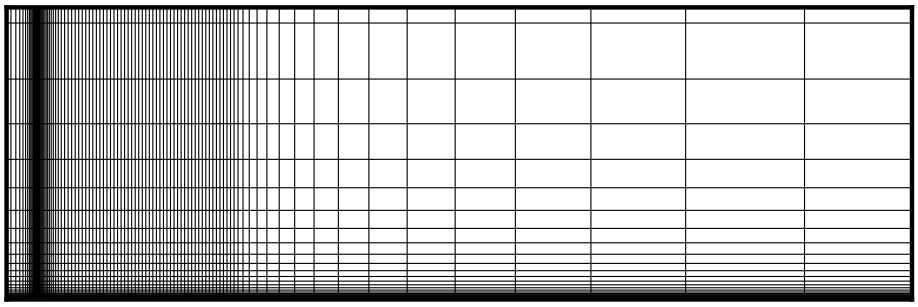

Figure 3: Computational mesh. Every second grid line is shown.

To judge the level of convergence the momentum and continuity equation residuals were scaled with momentum and mass flux through the inlet, respectively. Usually, when all scaled residuals reaches a level of 10^{-3} or lower the computations can be considered as being fully converged but, as will be illustrated later, these computations require extra care when judging convergence.

3.1 Comments on the test case used for validation

The main test cases considered for validation of the investigated models performance in transitional flows are the T3A and T3B cases used by the ERCOFTAC SIG on Transition coordinated by Prof. Mark Savill, presently at the Cranfield University. Both cases are considered zero pressure gradient flows over a flat plate and their only difference is the freestream turbulence intensity that in the T3A case is three percent and six percent in the T3B case. The experimental data was obtained at the Rolls-Royce Applied Science Laboratory. A schematic of the experimental rig is shown in Figure 4.

As can be seen from Figure 4 the plate in the experiment is not infinitely thin and has an apex shaped leading edge with a radius of 0.75 mm at the very beginning of the plate. To avoid laminar separation at the leading edge the plate in the experiment was inclined by about 0.5 degree.

A second set of data (Blair (1983)) was also used when validating the implementation of the Walters and Leylek (2004) model for transitional flows. These data are similar to the ERCOFTAC cases but the experimental set-up used allowed much larger turbulence length scales and can therefore be used as a complement to the ERCOFTAC data.

Important in CFD in general and in transition modelling in particular is to ensure that computed results are independent of numerical aspects such as mesh density and discretization, and that the boundary conditions are the same as in the experiment used for validation. The numerics will be considered in the section to follow and we will here address the geometrical and boundary condition

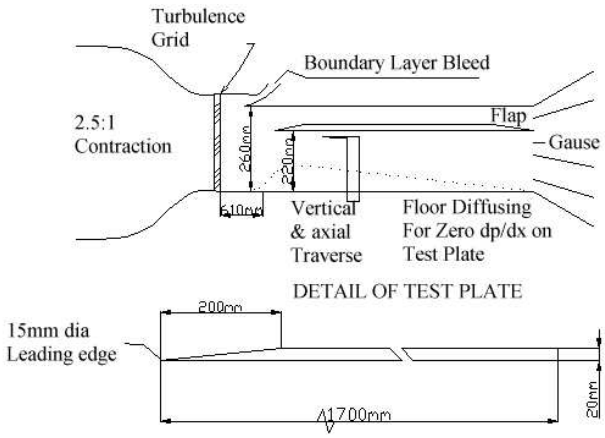

Figure 4: Schematic of T3A and T3B experimental set-up. Figure obtained from `http://cfd.me.umist.ac.uk/ercofold/database/test20/test20.html`

assumptions that possibly can affect the predicted transition process. The three most important ones are:

- The shape of the leading edge. In almost all earlier studies it is assumed that the real flat plate can be approximated with an infinitely thin plate. In experiments the plate is not very thin and usually has an apex with a rounded leading edge at the start of the plate (cf. Figure 4). Even though the edge radius is small it is not unlikely that it will have an effect on, for example, the production of turbulence energy at the leading edge.

  Whether or not the assumption that the plate is of zero thickness is of any importance is not investigated in this study. Worth mentioning, however, is that Roach (1992) compiled data from various experimental studies where different plate thicknesses were used. He found that the ratio of the length scale of the freestream eddies to the plate thickness had a surprisingly strong influence on the location of transition. Finally, in the computational work of Menter et al. (2004) a rounded leading edge is used, whereas in all other studies the author know of an infinitely thin plate has been used.

- Failure of achieving the same pressure (gradient) conditions as existed in the experiment. It is a well known fact that pressure gradients does affect transition; a favourable gradient delays the process whereas an adverse pressure gradient tends to accelerate it. In most flat plate measurements experimentalists do their very best in order to have zero pressure gradient conditions in the freestream. This is achieved by manipulating the wall opposite to the plate on which the measurements are taken[1]. Unfortunately, the exact

[1]The reason why this is not straightforward is that the growth of the boundary layers on the

details of how these conditions are achieved are never given but instead the flow is categorized as a flat plate zero pressure gradient flow. Further, it is not clear if the tilting of the flat plate itself affects the flow adjacent to it. The possible effects of these uncertainties can be investigated by increasing the height of the domain or by tilting one of the two the walls.

- The position of the inlet relative to the leading edge of the plate. Many investigations have showed that it is not adequate to have the inlet coinciding with the leading edge of the plate. Therefore the plate is preceded by a short region (cf. Figure 2) where a symmetry boundary condition is applied. This way most uncertainties regarding what conditions to specify at the inlet are avoided as constant profiles can be specified for all quantities involved and the flow will adjust as the flat plate is approached. However, it is not clear how long an upstream distance is needed for the flow to adjust to the new conditions without being influenced by the choice of this distance. Note that as soon as the flow senses the presence of the plate (via the pressure of elliptic nature) the flow will slow down/speed up, which may affect the predicted turbulence production.

In an effort to investigate the influence of small pressure gradients in the computations the lower no-slip wall or the upper slip wall (symmetry boundary) was inclined to produce favorable pressure gradients. Further, as the velocity in the experimental freestream above the plate is not constant but accelerates (cf. Figure 5) there must exist, even though it is probably small, a favorable pressure gradient in the freestream. Thus, a second objective was to find out whether or not the freestream acceleration could be attributed to either of the geometry modifications.

Figure 5 shows a comparison of the predicted and the measured freestream acceleration in terms of a local freestream velocity scaled with its inlet value. The computed values are taken at a constant height above the plate approximately equal to the boundary layer thickness at $Re_x = 6 \times 10^5$. Three cases are considered: the standard case (both walls horizontal), a case where the top (slip) wall is tilted about 6 degrees and a final case where the flat plate is tilted 2.5 degrees (note that the reported tilt in the experiment was 0.5 degrees). The results are compared with the T3A and T3B data. It can be seen that the freestream acceleration seen in the experiment most likely owes to an inclination of the flat plate itself as the trend of this test case at least qualitatively resembles that seen in the measurements. The deviation just downstream of the leading edge ($0 < Re_x < 2 \times 10^5$) is probably due to the finite thickness of the plate used in the experiment causing an acceleration around the rounded leading edge. Note also the blocking effect introduced with this modification. The effect of tilting the slip wall on the other hand does

plate and the wind tunnel walls acts as a contraction and the freestream fluid accelerates.

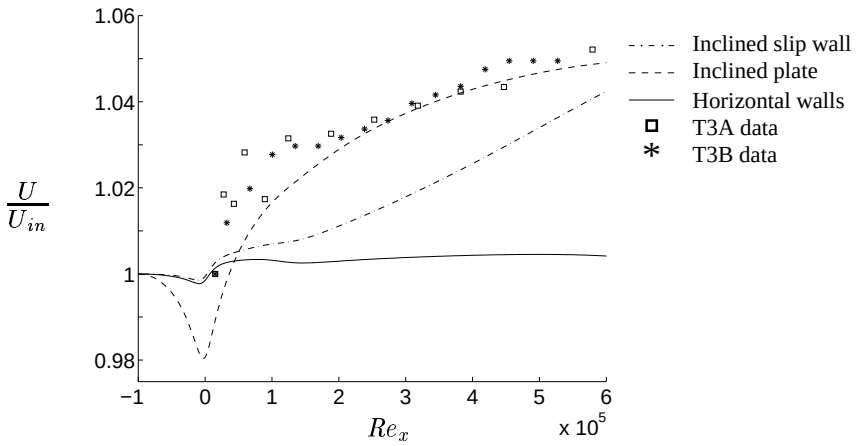

Figure 5: Freestream acceleration owing to the effect of inclined walls.

not couple with freestream acceleration in the experiment which indicates that the (unknown) shape of the opposite wall is of minor importance as compared with the tilting of the flat plate. Further, the result of the standard computation shows that the freestream acceleration, and thus the favorable pressure gradient, is small and therefore also that the extent of the domain normal to the plate is large enough to have essentially zero pressure gradient conditions. Finally, the small variation in velocity upstream of the leading edge indicates that the computational inlet is positioned sufficiently far upstream of the leading edge to prevent influence of the exact inlet position. Note however that this is not the case for the computation with the inclined flat plate.

The effect of tilting the slip wall on the transitional process was found to be negligible. There was however a small effect when the flat plate was inclined. This is illustrated in Figure 6 where C_f has been scaled with either the inlet velocity or the local freestream velocity. When scaled with the latter the curve collapses with the results of the standard case with the exception of the pretransitional region where a somewhat larger C_f is predicted. This suggests that the influence of the variations in freestream conditions seen in the experiment (and in the computations) is negligible and it is concluded that the T3A and T3B data may be compared with results of 'standard case' type computations.

3.2 Initial numerical study

Predicting by-pass transition requires the numerical scheme to predict diffusion of freestream turbulence energy into the boundary layer. As the location of transition has proved to be rather sensitive to the numerics used to mimic the phenomenon (Craft et al. (1997), Leschziner and Lien (2002)) an initial study was conducted in

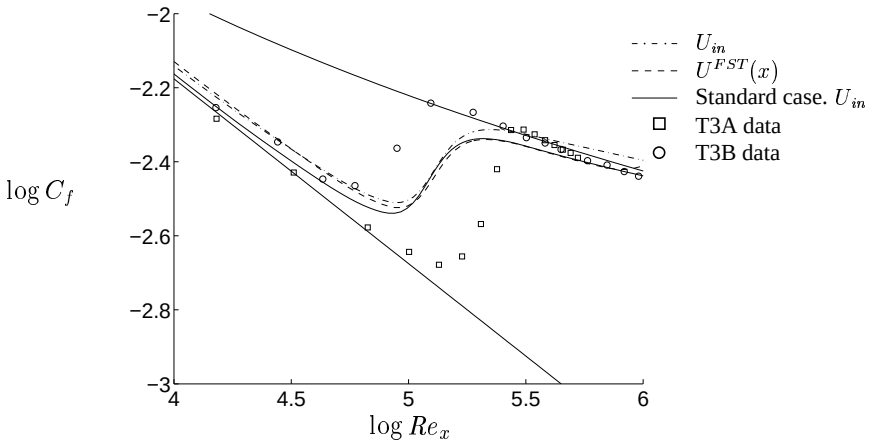

Figure 6: The effect of wall inclination on skin friction coefficient, C_f. C_f is for the tilted plate evaluated using two different scaling velocities.

order to find out how fine a grid is needed for the results to be grid independent. Also added are results of a computation on a domain of smaller physical size to see if the location of the slip wall or the outlet has any influence on transition.

Figure 7(a) plots the skin friction coefficient predicted with the $v^2 - f$ model for the T3B case ($Tu = 6.0\%$) as function of the local Reynolds number for three different meshes. They are referred to as fine (grid), coarse (grid) and small (domain). Also included are results at three intermediate stages in the iteration process. These stages are shown with circles in Figure 7 (b), where the convergence history for the refined mesh is plotted. As the (fully converged) results with all three grids give identical results they are regarded as being grid independent and not influenced by the actual domain size. Worth noting, however, is that the solutions show some sensitivity to the actual level of convergence. Therefore, throughout this study of transition on flat plates, extra care is taken to assure that the solutions are fully converged, or at least to make sure that the results of interest are not changing with increasing number of iterations.

A similar study was conducted for the three percent turbulence intensity case (T3A) as the freestream disturbances here are weaker as compared with the numerical 'disturbances' in the higher turbulence intensity case. It was found that an even finer mesh was required to have grid independent solutions and also that double precision computations were necessary. For convenience the mesh found suitable for the T3A case (cf. Figure 3) was used also for the T3B computations.

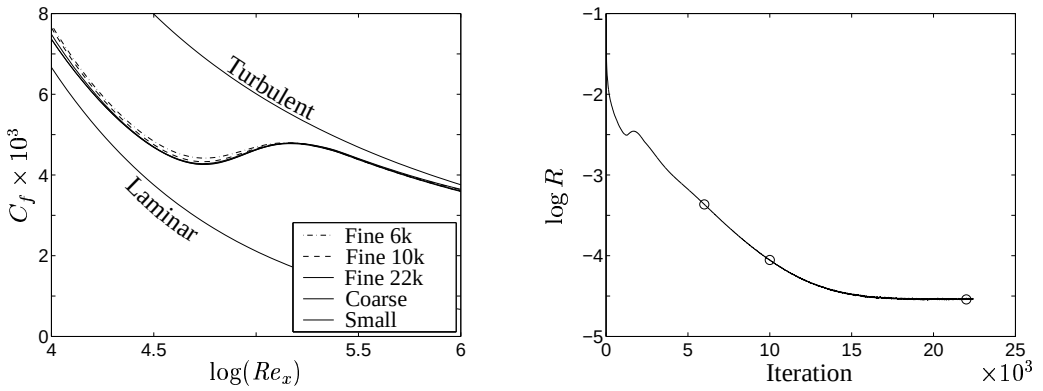

Figure 7: Left: predicted skin friction factor at three different convergence levels. Also included are results with the coarse mesh and smaller domain. Right: typical convergence history. Circles show at which convergence level the data to the left are plotted.

3.3 A note on numerical stability

During the investigation of possible mesh size influence it was found that the stability of the $v^2 - f$ model was not satisfactory. It turned out that some of the problems were related to the use of the realizability constraint[2], i.e. the time scale limit

$$T = \min\left(\frac{k}{\varepsilon},\ \frac{2k}{3C_{\mu 1}v^2}\frac{0.6}{\sqrt{S}}\right). \tag{29}$$

Surprisingly enough it turned out that the $v^2 - f$ model was much more stable in the flat plate computations when the realizability constraint was used. This was unexpected as the constraint decreases the predicted eddy diffusivity in the problem, which usually has a destabilizing effect. When switching the constraint off, that is, when the production of turbulence kinetic energy, and viscosity, was increased, the numerical properties of the scheme changed dramatically. To illustrate the instability of the $v^2 - f$ model (when implemented in the CALC-BFC framework) the U equation residual (normalized with inlet momentum flux) and the f equation residual (normalized with the f equation source term) are plotted in Figure 8. In this particular run the realizability constraint was inactivated and the under-relaxation factors used are also given in Figure 8 (note that they are low).

In the beginning of the iteration process the convergence is fine but at around 15,000 iterations some smaller peaks in the f residual appears. Immediately after

[2]Sveningsson (2003) showed that an upper bound on the turbulent time scale can cause numerical problems when used in the f equation. Hence the constraint is not applied in this equation.

one of these peaks the f residual abruptly goes up by a factor greater than 100. Soon thereafter the U residual and, although not shown here, all other variables follow and the results are no longer reliable.

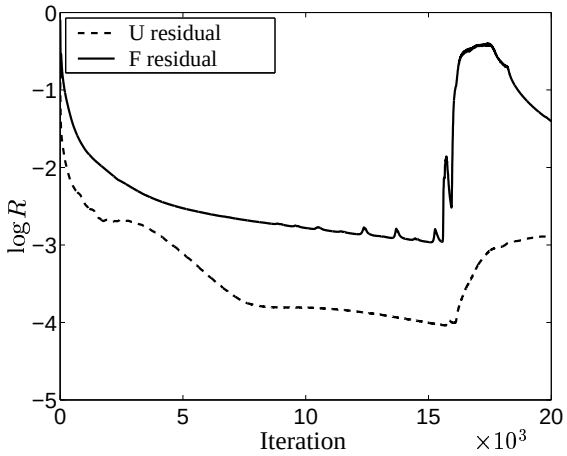

Variable	U, V	P	k, ε, v^2	f	μ_t
Relax. factor	0.3	0.15	0.2	0.05	0.4

Figure 8: Example of convergence history for a $v^2 - f$ computation on a 'coarse' mesh without use of the realizability constraint. The relaxation factors used are listed in the table.

Interesting to note is that the stability problems of the $v^2 - f$ model are reduced as the mesh density is increased. This was in fact one of the reasons why the finer mesh used for the T3A computations was employed also for the T3B computations, which in principle could have been performed on a much coarser mesh. Observations similar to this were made by Sveningsson (2003) in the mesh dependency study of the more complex flow around a stator vane linear cascade. Note also that Sveningsson and Davidson (2005) investigated the performance of the $v^2 - f$ model in a commercial software (Fluent) by implementing the model via so called user defined subroutines and found no problems in terms of poor convergence. Therefore it is the authors' belief that the numerical instabilities, when encountered, to a large extent is related to the ability of the flow solver, CALC-BFC, to handle computational meshes that are not optimally designed. As a more specific example some of our experiences suggest that large grid spacing at symmetry boundaries has a potential to cause problems. This has also been encountered by Petterson-Reif (private communication).

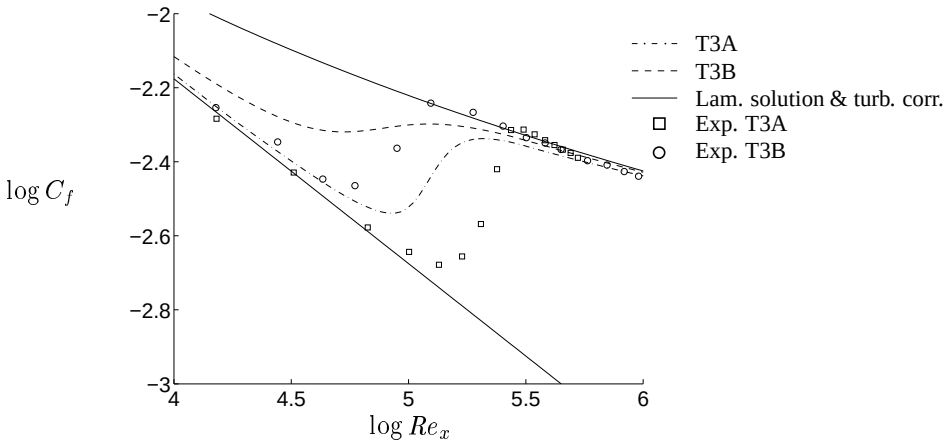

Figure 9: Response to elevated freestream turbulence of the $v^2 - f$ model.

4 Results

4.1 The Original $v^2 - f$ Model

As a first illustration of the fact that RANS turbulence models indeed have a potential to predict the influence of freestream turbulence on a transitional boundary layer the $v^2 - f$ model (Cokljat et al., 2003) is considered. Figure 9 shows a comparison of the predicted skin friction coefficients of the T3A and T3B cases with measured data. It can be seen that the model responds correctly to the increase in freestream turbulence as the point of transition onset moves upstream for the high turbulence intensity case. Another feature of the model is that the transition to turbulence is not as abrupt as often seen with typical two-equation turbulence models, but is preceded with a gradual increase in C_f that qualitatively resembles the trends seen in the experiment. The only problem, which indeed is the motivation for the present study, is that transition onset occurs far too early for both the high and low turbulence intensity cases. The results in Figure 9 were computed using a realizability constraint on the time scales appearing in the ε equation and the eddy-viscosity expression. The influence of the constraint in this flow, however, is almost negligible.

4.2 The Model of Walters and Leylek (2004)

To validate the implementation of the original LKE model the model was tested in a 1D fully developed turbulent channel flow ($Re = 395$). The predicted profiles of k_T, k_L, their sum and the predicted total dissipation rate ($\tilde{\varepsilon} + D_T$) are compared with the DNS of Kim et al. (1987) in Figure 10. It can be seen that the results agree well with the DNS. Further, the results are identical to those given in Walters and

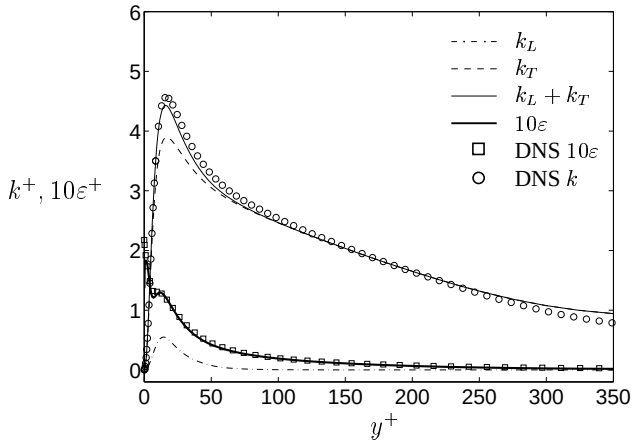

Figure 10: Profiles of fluctuating energies and dissipation rate ($\tilde{\varepsilon} + D_T$) in a fully developed turbulent channel flow. Results obtained with the model of Walters and Leylek (2004). Symbols show DNS data of Kim et al. (1987).

Leylek (2004). Thus it can be concluded that the fully turbulent behavior of the present implementation agrees with the original model.

To assess the implementation also in transitional flows the $Tu = 6.2\%$ and $Tu = 2.6\%$ freestream turbulence case of Blair (1983) is considered. This is the same data as was used by Walters and Leylek (2004) to validate their model. A comparison with the results in Walters and Leylek (2004) shows perfect agreement in both transition length and location which suggests that the implementation works well also in transitional flows. The predicted skin friction coefficients are shown in Figure 11 (dashed lines) but there is unfortunately no experimental skin friction data to compare with.

The reason behind the efforts to convince the reader that the implementation of the model is free from errors is that in the early stages of this study only the ERCOFTAC test cases T3A (flat plate $Tu = 3.0\%$) and T3B (flat plate $Tu = 6.0\%$) were considered. It turns out that the model of Walters and Leylek (2004) behaves very differently for these conditions as compared with the test cases of Blair (1983). This is illustrated in Figure 11 where the predicted skin friction coefficients are plotted for four different sets of freestream conditions (T3A, T3B, Blair 2.6% and Blair 6.2%). Also included are the experimental data for T3A (squares) and T3B (circles) together with the laminar solution (lower solid line) and a correlation for a fully turbulent boundary layer (upper solid line). Although not shown here the agreement of the computations with the two data sets of Blair (1983) is good with the exception of a slight overshoot just downstream of the location where the transition is completed and the model responds as expected to the increase in freestream turbulence level. The results for the ERCOFTAC data

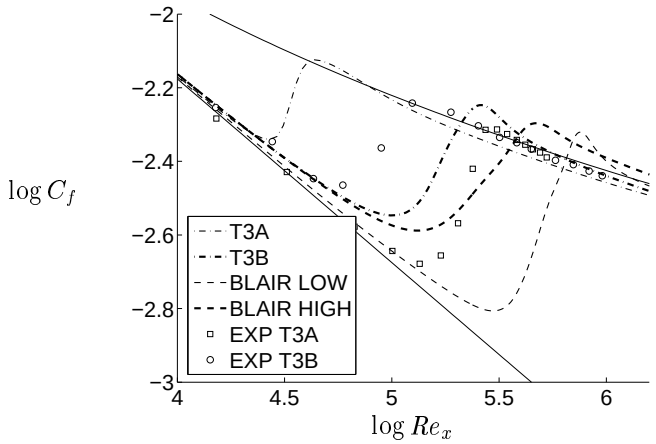

Figure 11: Streamwise development of the skin friction coefficient. The lower and upper solid lines are obtained from a laminar computation and a turbulent correlation, respectively.

sets on the other hand are much worse. For the T3B case ($Tu = 6\%$) transition is predicted to occur at $Re_x \approx 10^5$, which is almost a factor two later than observed in the experiment. For the T3A case the situation is even worse. Here the computed location of transition is $Re_x \approx 10^{4.4}$, which corresponds to a streamwise distance that is five times shorter than the measured value. Even more worrying is the fact that transition is predicted to occur earlier for the low turbulence intensity than for the higher turbulence intensity.

As the two turbulence levels from each of the two data sets are comparable the erroneous behavior of the model for the T3A and T3B cases must owe to a strong sensitivity to the prescribed freestream turbulence length scale, $\lambda_T = k_T^{3/2}/\varepsilon$. This length scale was found by matching the decay of turbulence kinetic energy in the freestream for the four different cases. The results of this matching procedure are shown in Figure 12 where the freestream TKE of the experiments are plotted together with the corresponding values of the simulations. The length scales producing the almost perfect matches are plotted in Figure 13, where it can be seen that the length scales of the T3A and T3B cases are considerably lower than in the computations of the Blair experiments.

The strong dependence on the freestream turbulence length scale is an undesired feature of the original LKE model. The dependence most likely stem from the procedure to compute the so called effective length scale, i.e.

$$\lambda_{\mathit{eff}} = \min\left(C_\lambda d, \lambda_T\right). \tag{30}$$

Here the wall distance d is of course independent of the freestream parameters whereas the turbulence length scale, $\lambda_T = k_T^{3/2}/\tilde{\varepsilon}$, is not. When the effective

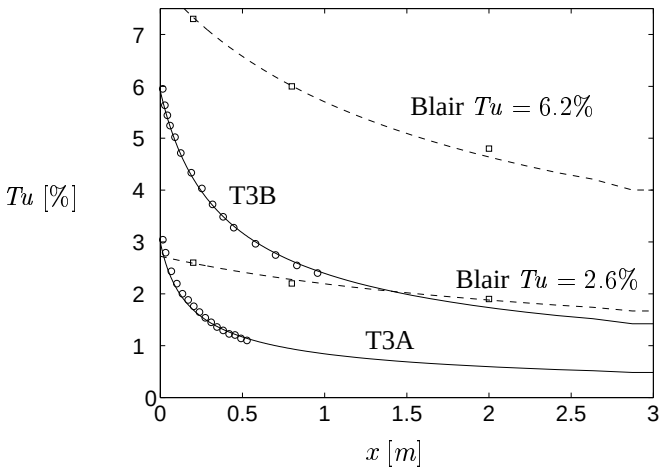

Figure 12: Comparison of measured and computed freestream decay of turbulence kinetic energy for the ERCOFTAC T3A and T3B test cases and the Blair (1983) $Tu = 2.6\%$ and $Tu = 6.2\%$ cases.

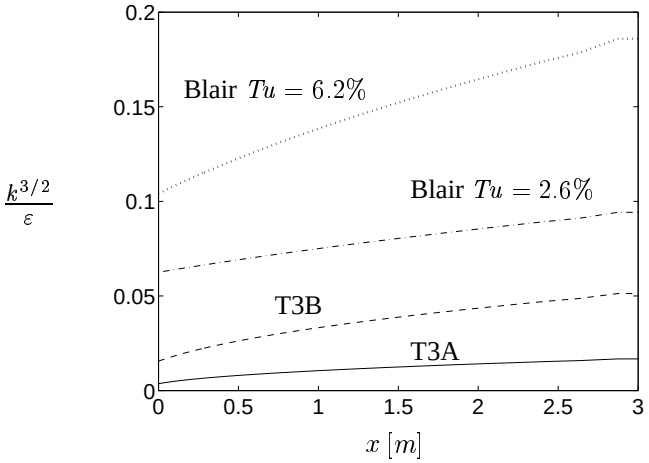

Figure 13: Computed freestream turbulence length scale, $k^{3/2}/\varepsilon$, for the ERCOFTAC T3A and T3B test cases and the Blair (1983) $Tu = 2.6\%$ and $Tu = 6.2\%$ cases.

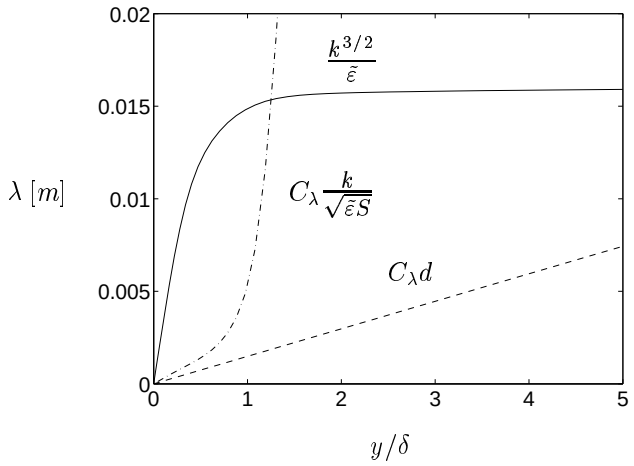

Figure 14: Profiles of the different length scales used to separate small scale energy from large scale energy. Results from case T3B obtained with the model of Walters and Leylek (2004) at $Re_x = 15,100$.

length scale is used to split up the TKE into its small and large scale parts (cf. Eqn 7) a decrease in $k^{3/2}/\varepsilon$ will lead to increasingly larger percentages small scale TKE. Consequently, as the small scale energy contributes to the production of TKE, this scenario has a potential to shorten the route to transition. In an effort to avoid having this problem also with the model suggested in the previous section the wall distance based length scale was replaced according to

$$\lambda_{\mathit{eff}} = \min\left(C_\lambda \frac{k}{\sqrt{\tilde{\varepsilon}S}}, \frac{k^{3/2}}{\tilde{\varepsilon}}\right). \tag{31}$$

Figure 14 plots the turbulence length scale together with the two different length scales used to split the energy into small and large scale parts as function of wall distance in boundary layer height units. It can be seen that when the wall distance based scale is used the intersection where the effective length scale switches to the turbulence length scale has no coupling to the extent of the boundary layer. Thus, a change in freestream length scale will have an effect on how far away from the wall the effective length scale will take its lower value. Under the circumstances shown in Figure 14 the switch occurs at $y/\delta \approx 10$ and the larger the turbulence length scale the further out switch takes place.

When using the length scale in Eqn 31 the switch always (at least in the flat plate case considered here) takes place at about the edge of the boundary layer. This construction is believed to reduce the sensitivity of the new model to the prescribed level of turbulence length scale in the freestream. Note, however, that a reduced length scale extending well beyond the boundary layer affects turbulence production also around stagnation points and will reduce the overproduction of TKE that is usually avoided with a realizability constraint.

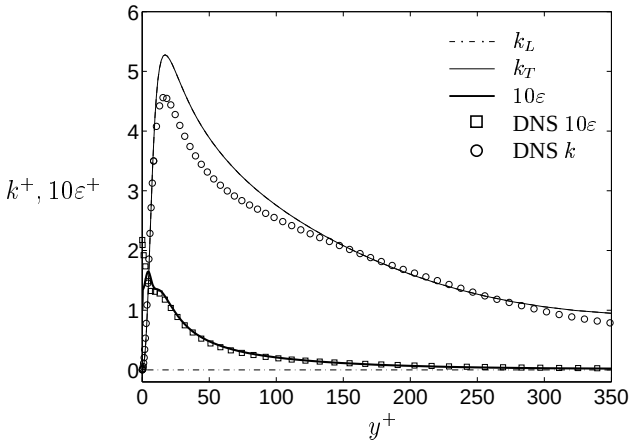

Figure 15: Profiles of fluctuating energies and dissipation rate ($\tilde{\varepsilon} + D_T$) in a fully developed turbulent channel flow. Results obtained with the modified $v^2 - f$ model. Symbols show DNS data of Kim et al. (1987).

4.3 The Modified $v^2 - f$ Model

The extension and modifications to the original $v^2 - f$ model suggested in Section 2 where first validated against the DNS data of Kim et al. (1987) in the fully developed turbulent channel flow. Figure 15 shows some results of this comparison. Included are profiles of the predicted laminar and turbulence kinetic energy (k_L and k_T) and the (total) dissipation rate of k_T. The k_T profile is close to that of the original $v^2 - f$ model (not included here) and the predicted ε profile follows the DNS data closely. Note also the similarity of the ε profile with that of the Walters and Leylek (2004) model (Figure 10). The main difference between the modified and the Walters and Leylek (2004) models is that the former predicts $k_L = 0$ throughout the channel whereas some LKE remains in the latter. This decoupling of the LKE from turbulent boundary layers was a desired feature that allows modifications of the LKE equation without modifying the behavior in turbulent boundary layers.

Finally, the modified $v^2 - f$ model was preliminary tested in a transitional flat plate flow. Figure 16 shows the development of the different components of the fluctuating energy together with a plot of the skin friction coefficient illustrating the state of the boundary layer. It can be seen that after an initial growth of laminar kinetic energy (not shown here as it occurs upstream of the location in Figure 16b) it begins to transform into turbulent kinetic energy (Figure 16c). Shortly after this initial growth in k_T the production of k_T, P_T, is triggered and the transition process accelerates. As k_T grows the function $f_{\mu,l}$ (cf. Eqn 18-20) rapidly goes to zero, which consequently forces to production of k_L to vanish as well. Without any additional production of k_L the R and D_L sink terms soon bring k_L to zero,

which indeed is the desired scenario. Note that the new model captures the slight overshoot at the later stages of the transition but that the transitional process is somewhat to rapid (cf. Figure 16a).

The model was also tested in the T3A test case where it failed to reproduce the growth of the laminar kinetic energy. As the growth of k_L was too small the production of k_T was not sufficiently dampened and transition was predicted to occur too early. This failure is likely due to the expression for the effective length scale and shows features similar to the failure of the Walters and Leylek (2004) model to predict the T3A and T3B cases. Thus, the expression for the effective length scale suggested in Eqn 8 is probably not suitable for flows where the freestream turbulence length scale is small (i.e. the same problem as with the Walters and Leylek (2004) model). In Figure 14 it can be seen that if the freestream length scale is small ($0.005m$ and smaller), the ratio of the effective to turbulence length scale is relatively large and only a limited amount of the turbulence kinetic energy becomes large scale energy (cf. 7), which contributes to production of k_L (cf. Eqn 10).

5 Concluding remarks

In this study the performance of two turbulence/transition models have been examined. The first model, suggested by Walters and Leylek (2004), was found to work reasonably well in two transitional flat plate flows in which the freestream turbulence length scale was relatively large. In two different test cases with smaller length scales the model's performance was considerably poorer, which suggests a strong length scale dependence of the model. The second model, developed in this paper, adopts many of the transition specific features of the Walters and Leylek (2004) model. The model is based on the $v^2 - f$ model and the overall aim of this study has been to couple the $v^2 - f$ model, which is known to perform well in turbulent flows, to the transition modelling approach of Walters and Leylek (2004) to improve the $v^2 - f$ model's performance in transitional boundary layer flows.

Initial computations with the new model illustrated the potential of solving an additional transport equation for a laminar fluctuating energy. The information on the pretransitional boundary layer carried by this equation was used to model the by-pass transition mechanism suggested by e.g. Jacobs and Durbin (2001), i.e. that laminar streaks in the fluctuating u velocity component eventually breaks down to form turbulent spots. Unfortunately, the new model inherited the sensitivity to the freestream length scale of the Walters and Leylek (2004) model and, thus, the measure to split the turbulent kinetic energy into small and large scale components must be revised.

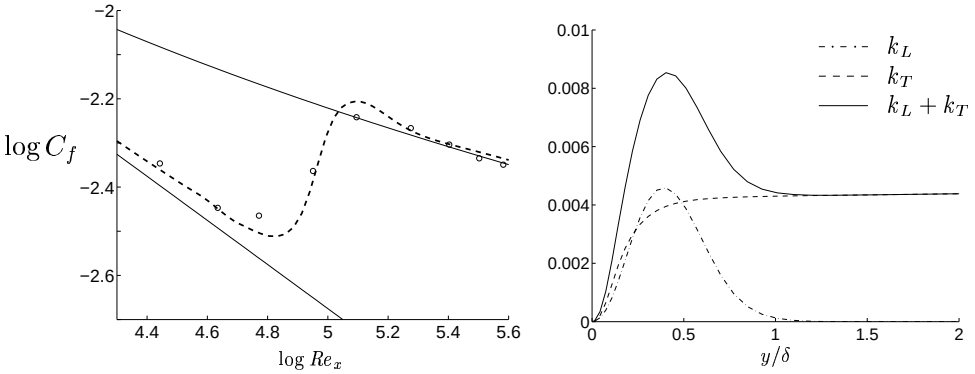

(a) C_f (b) $\log Re_x = 4.44$

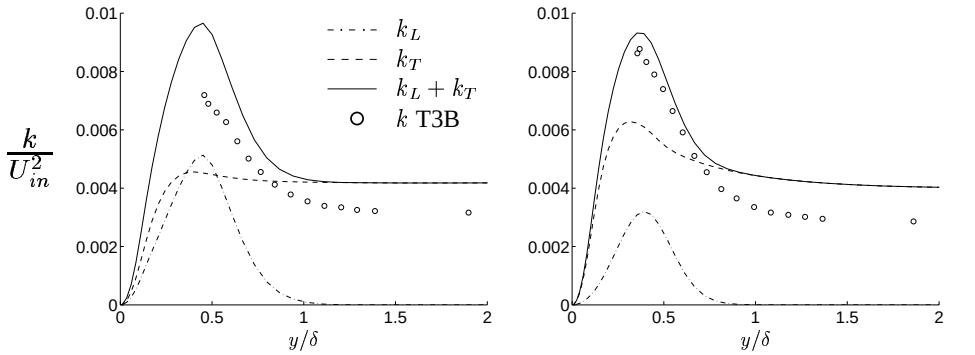

(c) $\log Re_x = 4.63$ (d) $\log Re_x = 4.77$

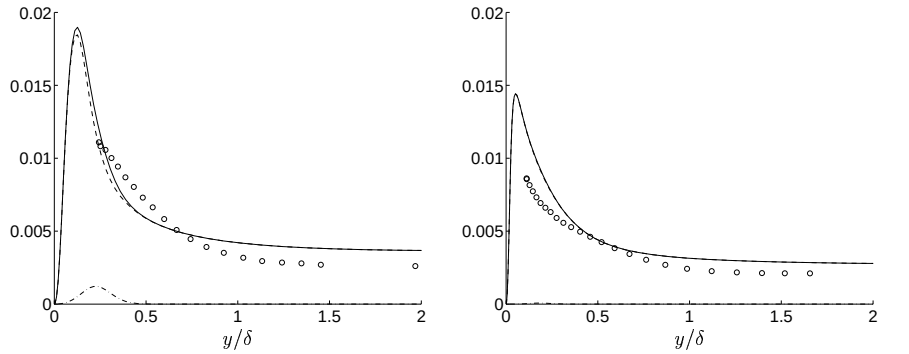

(e) $\log Re_x = 4.95$ (f) $\log Re_x = 5.27$

Figure 16: Boundary layer profiles of the fluctuating energy components at positions in the laminar, transitional and fully turbulent regions of the boundary layer. Circles show experimental data from the T3B test case.

References

Blair, M., 1983. Influence of free-stream turbulence on turbulent boundary layer heat transfer and mean profile development, part I–experimental data. Journal of Heat Transfer 105, 33–40.

Bradshaw, P., 1996. Turbulence modelling with application to turbomachinery. Proc. Aerospace Science 32, 575–624.

Brandt, L., Schlatter, P., Henningson, D. S., 2004. Transition in boundary layers subject to free-stream turbulence. Journal of Fluid Mechanics 517, 167–198.

Byggstoyl, S., Kollmann, W., 1981. Closure model for intermittent turbulent flows. Int. J. of Heat and Mass Transfer 24, 1811–1821.

Cokljat, D., Kim, S., Iaccarino, G., Durbin, P., 2003. A comparative assessment of the $\overline{v^2} - f$ model for recirculating flows. AIAA-2003-0765.

Craft, T., Launder, B., Suga, K., 1997. Prediction of turbulent transitional phenomena with a nonlinear eddy-viscosity model. Int. J. Heat and Fluid Flow 18, 15–28.

Davidson, L., Farhanieh, B., 1995. CALC-BFC: A finite-volume code employing collocated variable arrangement and cartesian velocity components for computation of fluid flow and heat transfer in complex three-dimensional geometries. Rept. 95/11, Dept. of Thermo and Fluid Dynamics, Chalmers University of Technology, Gothenburg.

Dopazo, C., 1977. On conditioned averages for intermittent turbulent flows. Journal of Fluid Mechanics 81, 433–438.

Durbin, P., 1991. Near-wall turbulence closure modeling without 'damping functions'. Theoretical and Computational Fluid Dynamics 3, 1–13.

Jacobs, R., Durbin, P., 2001. Simulations of bypass transition. Journal of Fluid Mechanics 428, 185–212.

Kim, J., Moin, P., Moser, R., 1987. Turbulence statistics in fully developed channel flow at low Reynolds number. Journal of Fluid Mechanics 177, 133–166.

Lardeau, S., Leschziner, M., Li, N., 2004. Modelling bypass transition with low-reynolds-number nonlinear eddy-viscosity closure. Flow, Turbulence and Combustion 73, 49–76.

Lardeau, S., Li, N., Leschziner, M., 2005. LES of transitional boundary layer at high free-stream turbulence intensity, and implications for RANS modelling. In: 4th Int. Symp. on Turbulence and Shear Flow Phenomena. pp. 431–436.

Leschziner, M. A., Lien, F. S., 2002. Numerical aspects of applying second-moment closure to complex flows. In: Launder, B. E., Sandham, N. D. (Eds.), Closure Strategies for Turbulent and Transitional Flows. Cambridge University Press, pp. 153–187.

Mayle, R., Schultz, A., 1997. The path to predicting bypass transition. Journal of Turbomachinery 119, 405–411.

Menter, F., Langtry, R., Likki, S., Suzen, Y., Huang, P., Volker, S., 2004. A correlation based transition model using loacal variables part I – model formulation. In: ASME Turbo Expo 2004. Paper no. GT-2004-53452.

Pettersson-Reif, B. A., Durbin, P. A., Ooi, A., 1999. Modeling rotational effects in eddy-viscosity closures. International Journal of Heat and Fluid Flow, 563–573.

Radomsky, R., Thole, K., 2001. Detailed boundary layer measurements on a turbine stator vane at elevated freestream turbulence levels. Journal of Turbomachinery 122, 666–676.

Roach, P. E., 1992. A correlation analysis approach to the T3 test case. In: Pironneau, O., Rodi, W., Ryhming, I. L., Savill, A. M., Troung, T. V. (Eds.), Numerical Simualtion of Unsteady Flows and Transition to Turbulence. Cambridge University Press, pp. 348–354.

Savill, A. M., 2002a. By-pass transition using conventional closures. In: Launder, B. E., Sandham, N. D. (Eds.), Closure Strategies for Turbulent and Transitional Flows. Cambridge University Press, pp. 464–492.

Savill, A. M., 2002b. New strategies in modelling by-pass transition. In: Launder, B. E., Sandham, N. D. (Eds.), Closure Strategies for Turbulent and Transitional Flows. Cambridge University Press, pp. 493–521.

Steelant, J., Dick, E., 1996. Modelling of bypass transition with conditioned navier-stokes equations coupled to an intermittency transport equation. International Journal of Numerical Methods in Fluids 23, 193–220.

Sveningsson, A., 2003. Analysis of the performacne of different $\overline{v^2} - f$ turbulence models in a stator vane passage flow. Licentiate thesis, Dept. of Thermo and Fluid Dynamics, Chalmers University of Technology, Gothenburg, Sweden.

Sveningsson, A., Davidson, L., 2005. Computations of flow field and heat transfer in a stator vane passage using the v^2-f turbulence model. Journal of Turbomachinery 127, 627–634.

Walters, D., Leylek, J., 2004. A new model for boundary layer transition using a single-point rans approach. Journal of Turbomachinery 126, 193–202.

Westin, K. J. A., Henkes, R. A. W. M., 1997. Application of turbulence models to bypass transition. Journal of Fluids Engineering 119, 859–866.